

Electrodeposition of Nickel-Molybdenum Nanoparticles for Their Use as Electrocatalyst for The Hydrogen Evolution Reaction

M. Videa^{1,*}, D. Crespo¹, G. Casillas² and G. Zavala²

¹Department of Chemistry, Tecnológico de Monterrey Campus Monterrey,

²Department of Physics, Tecnológico de Monterrey Campus Monterrey,
Av. E. Garza Sada 2501, 64849 Monterrey, N.L., México.

Received: November 11, 2009, Accepted: February 02, 2010

Abstract: Nickel-Molybdenum nanoparticles are produced using current pulses to electrodeposit alloys from a NiSO_4 , Na_2MoO_4 and $\text{Na}_3\text{C}_6\text{H}_5\text{O}_7$ electrolytic bath. Glassy carbon discs of 1mm and 2.5mm diameter and carbon felt are used as working electrodes. The electrocatalytic activity of the deposits for Hydrogen Evolution reaction (HER) was evaluated from measurements of the currents obtained when performing cyclic voltammetry experiments on a 0.72 M H_2SO_4 electrolyte. From Tafel plots a Volmer Heyrovsky mechanism can be inferred. The deposits on glassy carbon electrodes were inspected by atomic force microscopy (AFM) revealing particles with diameters between 25 to 120 nm. SEM was used to confirm the electrodeposition of NiMo on carbon felt fibers. At high current density pulses deposits with good catalytic properties for HER are obtained.

Keywords: electrocatalysis, NiMo alloys, nanoparticles, HER.

1. INTRODUCTION

In recent years hydrogen has acquired great interest as an energy carrier and a promising fuel to replace current fossil fuels considering the imperative need of an active strategy to reduce the environmental effects of atmospheric CO_2 accumulation [1]. In this respect, electrolysis of water is becoming the alternative of choice to generate hydrogen as long as it is ensured that the energy used in its production comes from a source which is at least carbon neutral [2]. Nevertheless, several technological constraints as well as cost limitations have delayed its implementations towards a hydrogen economy. Among them, the current use of expensive and scarce metals such as platinum has prompted us to investigate the possibility of new materials made from earth-abundant elements and with electrocatalytic properties similar to those of platinum [3].

Nickel Molybdenum (NiMo) alloys have shown good corrosion resistance and electrocatalytic activity for the hydrogen evolution reaction that considerably surpass those of their individual components, a phenomenon that has been named synergetic effect [4-6]. Because of this, several studies have been devoted to the synthesis

and optimization of characteristics of the alloy such as composition, surface area, morphology of the deposit and particle size. Electrodeposition is frequently selected as the method to prepare Ni-Mo alloys because it allows the control of the grain size of the deposit at low temperatures avoiding the formation of oxides. In particular, synthesis of materials with nanometric dimensions has been studied by Schulz and Huang who report the relation between nanocrystalline structure and electrocatalytic activity of NiMo alloys [7,8]. In the present work we report the electrochemical synthesis of NiMo nanoparticles directly on the surface of glassy carbon and carbon felt electrodes under galvanostatic control, offering an alternative method to the preparation of the NiMo alloys. The catalytic activity of the deposits was evaluated from measurements of the currents obtained when performing cyclic voltammetry experiments on a 0.72M H_2SO_4 electrolyte. The deposits were inspected through electron microscopy and atomic force microscopy (AFM).

2. EXPERIMENTAL

All experiments were carried out in an EG&G PAR Potentiostat/Galvanostat model 273A with a computer interface. A three-electrode cell was built using a platinum net and a home-made

*To whom correspondence should be addressed: Email: mvidea@itesm.mx
Phone: (81)83284489, fax (81)81582024

calomel electrode (0.242 V vs. NHE) as counter and reference electrode, respectively. The reference electrode was placed in glass tube with a Luggin capillary tip. Glassy carbon rods (Alfa Aesar) and carbon felt (Aldrich) were used to build the working electrodes.

Glassy carbon rods of 1 mm or 2.5 mm diameter (geometric areas of ca. $7.8 \times 10^{-3} \text{ cm}^2$ and $49 \times 10^{-3} \text{ cm}^2$, respectively) were introduced in a glass tube filled with epoxic resin. In order to have electric connectivity a mercury plug was used as contact and a copper wire. Paraffin was used as a sealant over the mercury contact. Previous to any experiment, the surface of the electrode was cleaned with 90% HNO_3 and polished with abrasive paper and 1.0, 0.3 and $0.1 \mu\text{m}$ alumina. Finally, the electrodes were washed with acetone and deionized water. The electrolytic bath solution had the following composition: 0.2 M $\text{Ni}_2\text{SO}_4 \cdot 6\text{H}_2\text{O}$ (PQM), 0.06 M $\text{Na}_2\text{MoO}_4 \cdot 2\text{H}_2\text{O}$ (Mallinckrodt) and 0.136 M $\text{Na}_3\text{C}_6\text{H}_5\text{O}_7 \cdot 2\text{H}_2\text{O}$ (Baker); a pH of 9.0 was adjusted adding ammonium hydroxide. All solutions were prepared using deionized water.

As a means of characterization of the initial activity of the 'naked' glassy carbon electrodes before the NiMo electrodeposition a cyclic voltammetry was carried out in a solution of sulfuric acid 0.72 M at a scan rate of 2 mV s^{-1} from the open circuit potential to -0.5 V vs. SCE . Then the NiMo deposits were electrochemically prepared using current pulses. In order to assess the correlation between the total charge used in the preparation of the deposit and its electrocatalytic activity, several experiments were performed using a fixed current density of $42 \text{ mA} \cdot \text{cm}^{-2}$ at pulse times of 90, 312, 632, 2500 and 5000 ms, respectively. The influence of current density of the pulses was also studied by maintaining a constant charge of $165 \mu\text{C}$ using density currents of 10, 40, 70, 100 and $200 \text{ mA} \cdot \text{cm}^{-2}$, respectively.

Some earlier experiments were also conducted on disk electrodes of glassy carbon which were designed in order to allow the inspection of the deposits using Atomic Force Microscopy. The electrical contacts to these discs were made with silver paint and sealed with silicone glue to limit the contact of the solution to the cross section of a glassy carbon exposed. The cleaning process for these electrodes was similar to that of the glassy carbon electrodes described above. Additionally, we evaluated the use of carbon felt, comprising intertwined carbon fibers, as an ideal substrate for the deposition of NiMo due to its large surface area, low cost and high stability. The electrodes of this material were prepared by cutting $0.5\text{cm} \times 3\text{cm}$ pieces held at one end with an alligator clip. Previous to any experiment the carbon felt was immersed in deionized water and subjected to an ultrasonic bath, then was dried at 60°C . During the experiments approximately 2cm from the electrode is immersed in the electrolyte solution. Cyclic voltammetry experiments were carried out in the electrolytic bath; the potential sweep was done from 0.055 V to -1.400 V vs. SCE at a scan rate 50 mVs^{-1} . Experiments were also made through direct current pulses of 40, 60, 80, 120, 160 and 220 mA, and with application of multiple pulses. The resulting deposits were inspected using scanning electron microscopy. The surface topography of the glassy carbon electrodes was characterized after the electrodeposition using a Veeco Atomic Force Microscope NanoScope Multimode IIIa in tapping mode with silicon tips. The images of scanning electron microscopy were obtained using the technique of backscattered electrons in an electron microscope FEI XL-30.

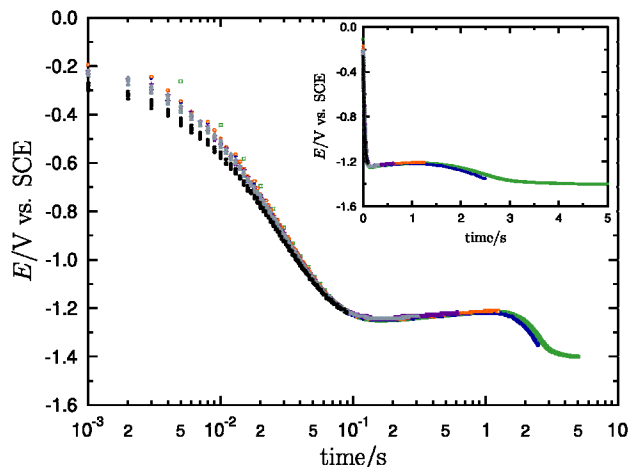


Figure 1. Electrode potential during a current pulse of a current density of $42 \text{ mA} \cdot \text{cm}^{-2}$. The chronopotentiometric curves of several experiments with pulse times of 90ms, 311ms, 623ms, 1.25s, 2.5s and 5s show similar behavior, reaching -1.2 V at 0.1s and showing a second drop to -1.4 V at around 1.5s. At the longest time the final potential of the electrode remains constant at this voltage. Notice that the time scale is logarithmic in order to show the polarization at shorter times. The inset shows the experiment results in linear time scale.

3. RESULTS AND DISCUSSION

Figure 1 shows chronopotentiometric curves obtained when a current density of $42 \text{ mA} \cdot \text{cm}^{-2}$ is applied during different periods of time. This current density is selected because it ensures that no molybdenum oxides will be present in the deposit [11]. The curves shown superimpose each other, suggesting the reproducibility of electrochemical processes occurring on its surface. In a first stage, within the first 200 ms there is a marked polarization of the electrode until a potential of -1.250 V vs. SCE is reached. Later we see a slight increase in the potential to -1.210 V vs. SCE , which extends approximately 1.5 seconds, giving rise to a second decrease in potential until nearly constant value of -1.380 V vs. SCE is reached. Videa reported a similar observation nickel deposit on ITO by current pulses [9]. According to that work, during the first stage of polarization, called variable phase, the potential reaches a sufficiently negative value that facilitates the formation of nuclei on the electrode surface at a speed imposed by the current density. In the next phase (stabilization phase) now nickel is deposited on the nuclei already formed, leading to particle growth, which occurs at a potential more positive than the first stage, since this process requires less overpotential and corresponds to the stabilization of the steady state.

To interpret the presence of additional stages in the results of this work (Figure 1) it is necessary to take into account that the ammonia-citrate bath is a complex system in which several chemical species coexist, with some of these forming electroactive complexes. In addition, four reactions at the cathode can take place: i) hydrogen evolution, ii) reduction of molybdate ion to lower valence oxides, ii) reduction and deposition of Ni and iv) deposition of

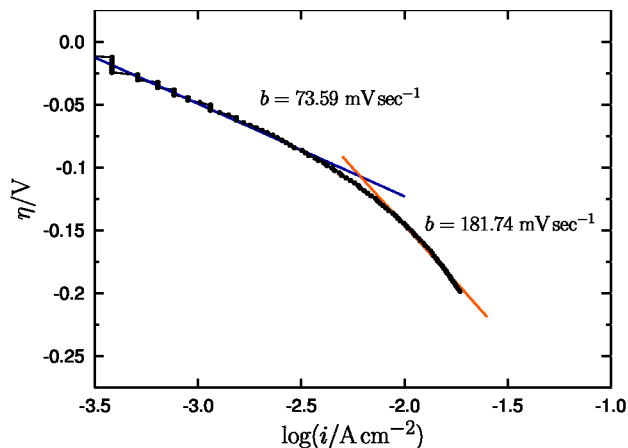


Figure 2. Tafel plot for hydrogen evolution. Two regions can be identified in accordance to a Volmer Heyrovsky mechanism. Typical values at low current densities are around -70mV dec^{-1} (continuous line) which changes at higher current densities to reach values close to -180mV dec^{-1} (dashed line).

NiMo [10]. According to Kuznetsov, NiMo alloy can be obtained only at potentials more negative than -1.17 V vs. SCE , which suggests that by reaching a potential of -1.250 V vs. SCE the first centers of NiMo are already formed. Then, as the nuclei grow, a second decrease in the potential may be associated with the depletion of electroactive species in the closest region to the electrode, such as the complex ion $[\text{Ni}(\text{HCit})(\text{NH}_3)_3]^-$ whose reduction potential is much more positive than of any of the complex ions formed by the citrate ion [11].

In order to evaluate the catalytic ability of the deposits, the apparent exchange current density, j_0 , and Tafel slopes were calculated from the results of cyclic voltammetry experiments in order to evaluate the kinetic characteristics of the hydrogen evolution reaction (HER) in a $0.72\text{M H}_2\text{SO}_4$ solution. The magnitude of this value is directly proportional to the electrocatalytic activity of the material. Two regions can be observed in accordance to a Volmer Heyrovsky mechanism, which is described by two consecutive steps: the reduction protons and adsorption of atomic hydrogen and the formation of an adsorbed molecule of hydrogen after the reduction of a second proton, as shown below:



An example is shown in Figure 2. The average experimental values obtained for each region are summarized in Tables 1 and 2. The values of the Tafel slopes obtained in this study are similar to those reported by Highfield [12].

The values shown in Table 1 suggest that longer current pulses produce deposits with slightly higher electrocatalytic activity for hydrogen evolution. It should be noted that the catalytic activity of the deposits obtained will depend on i) the amount of material deposited in proportion to the load, resulting in a greater number of active sites for the electrocatalysis of hydrogen evolution reaction, ii) the size of the particles deposited, iii) the morphology of the deposits and iv) the composition of the material obtained, all of which play a combined role [7,9]. The catalytic activity of the deposits increases with the pulse time and therefore the amount of deposited NiMo alloy consistent with point i). The current obtained at an overpotential, η , of -100 mV seems to follow a similar trend, being the highest at pulse time of 5 seconds.

The potential response of working electrode after applying cur-

Table 1. Apparent exchange current and current density at an overpotential of -100 mV for deposits obtained at different pulse times. The Tafel slopes at the two sections are presented.

Pulse Duration /ms	$\log j_0/\log(\text{A}\cdot\text{cm}^{-2})$	Current density / $\text{mA}\cdot\text{cm}^{-2}$ at $\eta=100\text{mV}$	Tafel slope first section / mV dec^{-1}	Tafel slope second section / mV dec^{-1}
90	-3.79 ± 0.11	4.04 ± 1.58	-77.84 ± 14.89	-150.73 ± 9.99
311	-3.63 ± 0.07	4.76 ± 1.63	-75.68 ± 11.83	-160.65 ± 12.26
623	-3.62 ± 0.09	5.09 ± 2.14	-75.10 ± 12.83	-162.48 ± 12.85
1250	-3.60 ± 0.09	4.99 ± 2.07	-77.06 ± 10.59	-161.11 ± 8.94
2500	-3.57 ± 0.10	4.73 ± 2.08	-80.10 ± 12.82	-166.57 ± 4.48
5000	-3.58 ± 0.14	5.39 ± 1.55	-74.13 ± 7.44	-163.54 ± 12.16

Table 2. Exchange current and current density at an overpotential of -100 mV during for hydrogen evolution on NiMo deposits prepared at different current densities. The final potential reported in the second column corresponds to the last value reached during the electroplating experiment.

Current density / $\text{mA}\cdot\text{cm}^{-2}$	Final Potential/V	$\log j_0/\log(\text{A}\cdot\text{cm}^{-2})$	Current density / $\text{mA}\cdot\text{cm}^{-2}$ at $\eta=-100\text{mV}$	Tafel slope first section / mV dec^{-1}	Tafel slope second section / mV dec^{-1}
10	-1.13 ± 0.01	-4.55 ± 0.13	0.25 ± 0.10	-112.87 ± 16.54	—
40	-1.21 ± 0.01	-3.74 ± 0.13	4.41 ± 0.95	-71.66 ± 10.12	-156.57 ± 15.16
70	-1.31 ± 0.02	-3.68 ± 0.06	3.32 ± 1.11	-81.35 ± 11.00	-164.03 ± 4.24
100	-1.38 ± 0.02	-3.81 ± 0.14	3.58 ± 0.58	-71.66 ± 21.38	-142.97 ± 16.57
200	-1.59 ± 0.03	-3.74 ± 0.19	4.89 ± 1.56	-67.81 ± 6.59	-142.29 ± 11.8

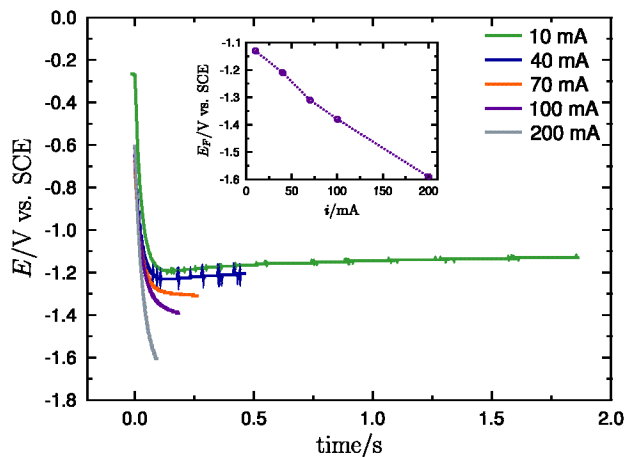


Figure 3. Electrode potential response during the application of pulses of different current densities and pulse time keeping a constant charge of $146 \mu\text{C}$. Several superimposed experiments of current densities ranging from 10 to $200 \text{ mA}\cdot\text{cm}^{-2}$ are shown. The inset shows a close to linear relation between the current pulse and the final potential attained.

rent densities of different magnitude maintaining a constant charge of $146 \mu\text{C}$ is shown in Figure 3. At higher current densities a rapid polarization of the electrode is observed and therefore a greater number of active sites for nucleation of metal particles resulting in a high density of particles may be expected [9].

In Table 2 we report the values of exchange current density, j_0 , obtained for HER using the deposits prepared using several current pulses. It can be observed that there is a marked effect on the current density in the catalytic activity of the deposits, with a difference of one order of magnitude between the experiments at 10 and $200 \text{ mA}\cdot\text{cm}^{-2}$, respectively. These differences in activity for the HER electrocatalysis are related to the four factors mentioned

above. It is also important to consider that although the amount of charge supplied in all cases is the same, it is likely that the coulombic efficiency decreases with increasing current density, as reported by Chassaing [13], since the overpotentials at which the Nickel deposits coincide with the potential of hydrogen evolution. Nevertheless, the electrocatalytic activity of the deposit is considerably higher. In fact, in the case of nickel electrodeposition, Penner has reported that hydrogen coevolution is a factor limiting the growth of particle sizes ranging between 20 and 600 nm and thus the overpotential can be used to select the size average particle [14]. The applied current density also has an influence on the resulting alloy composition and it is expected that at larger current pulses the concentration of molybdenum in the alloy will decrease [5,15]. The inset in Figure 3 shows a close to linear relationship between the current pulse and the final potential attained.

The inspection of the deposits was made on disk-shaped electrodes (Figure 4a). The AFM image acquired under tapping mode shows the result obtained for a deposit generated by a pulse of $200 \text{ mA}\cdot\text{cm}^{-2}$ for 92ms. The results in Figure 4b confirm that the deposited material is nanostructured and the particles have sizes in a range between 25 and 160 nm.

Carbon felt electrodes were used as substrates for electroplating particles of NiMo. The curves obtained in cyclic voltammetry experiments (Figure 5a) reveal that the carbon felt has a behavior similar to that reported by Crousiert for glassy carbon [16]. In both cases, there is no significant current until, in the case of felt, the potential reaches -1.1 V vs. SCE ; from this point the current increases rapidly. In the reversal of the polarization larger cathodic currents are observed until a zero current value at -0.763 V vs. SCE is reached.

The chronopotentiometric curves for several current pulses are shown in Figure 5.b. It can be seen a marked polarization, reaching electrode potentials below -1.4 V vs. SCE from current values of 40mA. There is a slight recovery potential of 200 mV and then acquire a stable potential. This may be due to the complexity of the active surface of carbon felt; to be composed of a large number of

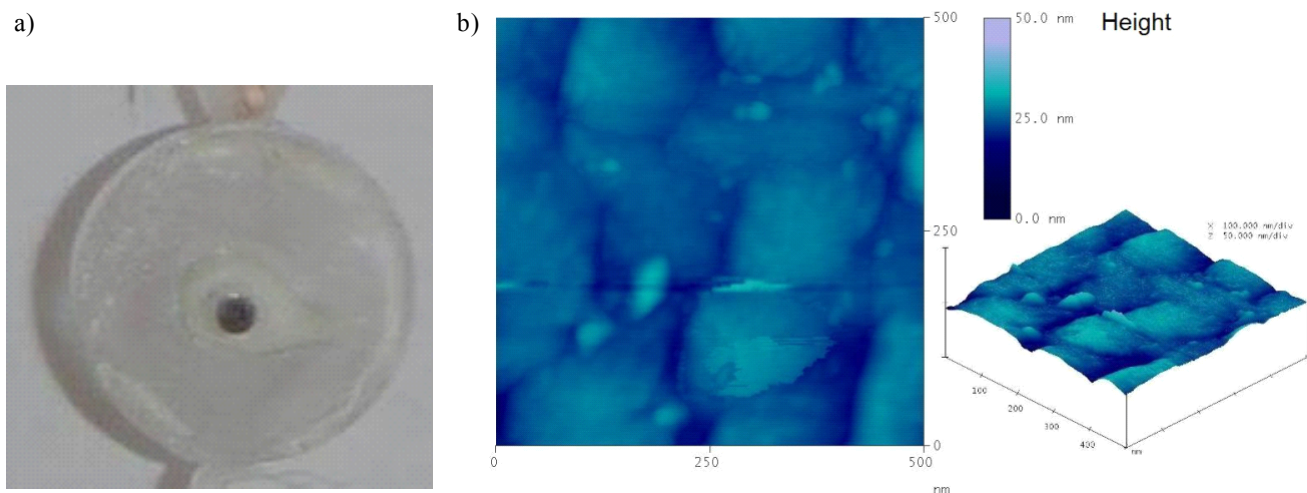


Figure 4. a) Electrode glassy carbon disk used inspection of the NiMo deposits with AFM microscopy. b) AFM micrographs for a NiMo deposit at a scale of 500 nm.

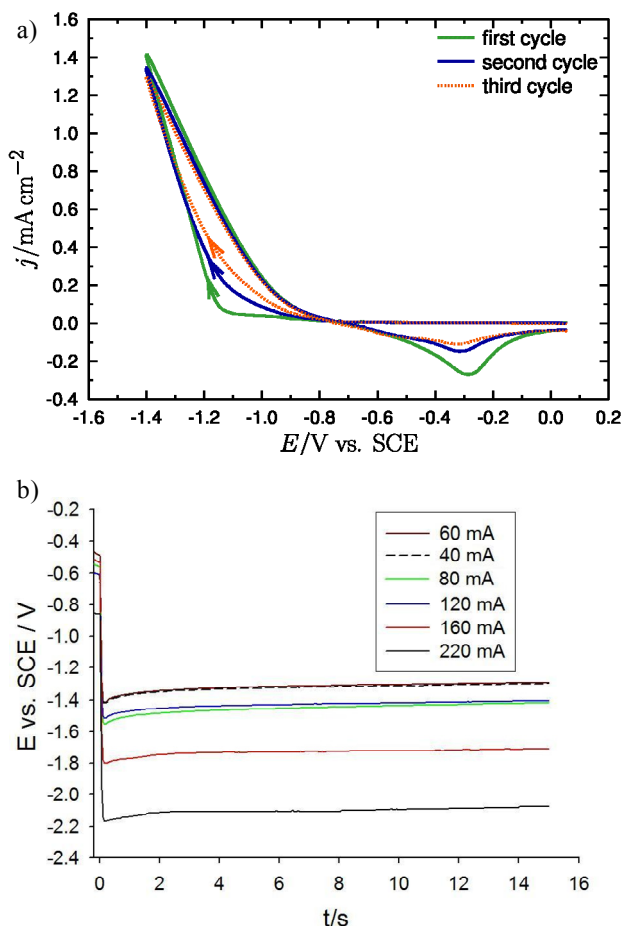


Figure 5. a) Cyclic voltammety performed using a carbon felt working electrode in a bath of 0.2 M Ni^{2+} , 0.06 M MoO_4^{2-} , 0.136 M sodium citrate adjusted to pH 9.0 with NH_4OH after consecutive cycles on a single electrode b) Behavior of the potential for electrodeposition on carbon felt using different current pulses.

fibers has considerable surface area and a distribution of sites with different activity in which they can carry out the reactions. The electrode potential reflects an average of the potentials of these reactions and it is therefore not possible to differentiate the processes observed for glassy carbon electrodes.

Figure 6a shows the results of an experiment in which consecutive pulses of 300 mA were applied, the first two of 10000 ms and a final 100 ms. It may be noted that during the second pulse electroplating potential is constant at -3.20V and no minimum appears, suggesting the growth of the alloy on the deposit formed during the first pulse is the only process occurring during this current pulse. Figure 6b corresponds to the scanning electron micrographs of NiMo deposit obtained after three pulses of current. One can see the formation of a uniform metal deposit on the fibers of felt and an area that clearly shows the formation of a discrete deposit. The presence of these particles is evidence that there is a nucleation mechanism for the electrodeposition of Ni-Mo alloy. EDS analysis confirmed the presence of Ni and Mo in the material deposited (not shown).

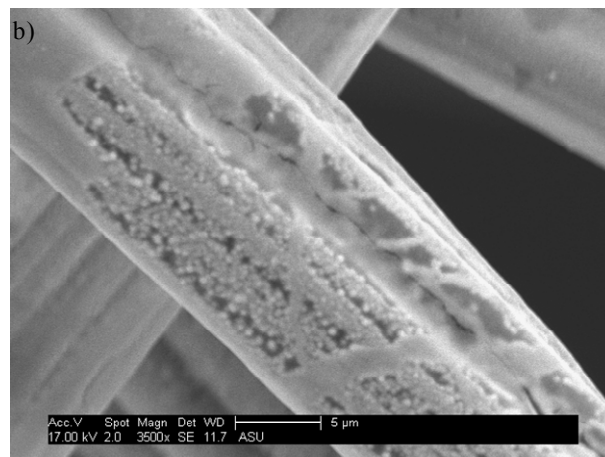
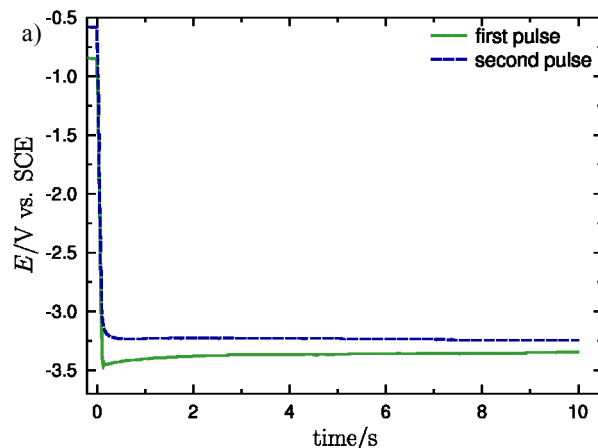


Figure 6. a) Chronopotentiometric behavior of the carbon felt electrode potential during the electrodeposition consecutive current pulses. b) Deposit on carbon felt produced after 2 pulses of 300 mA of 10 seconds.

4. CONCLUSIONS

We have successfully modified the surfaces of glassy carbon and carbon felt electrodes by electrodeposition of NiMo nanoparticles. These deposits show electrocatalytic activity which is related to the intensity of the current pulses used. However, because the activity depends on various factors is difficult to assign a single reason for the changes in catalytic ability and only apparent activity can be assigned to the calculated values of exchange current densities. Inspection further studies should be done. Despite this, it is clear that the use of high current density pulses of short duration generate deposits with good catalytic properties for HER. The electrodeposition of NiMo on carbon felt has been demonstrated and it is therefore possible to use this material as a substrate for the preparation of an electrode with a large active area and low cost.

5. ACKNOWLEDGEMENTS

The authors acknowledge the support provided by Tecnológico de Monterrey, Campus Monterrey through CAT-120 funds for the Chair of Nanomaterials and QUI019 and Dr. Sisouk Phrasavath from Arizona State University for the electron micrographs.

REFERENCES

- [1] N.S. Lewis and D.G. Nocera, PNAS, 103, 15729 (2006).
- [2] W. Vielstich; A. Lamm; H.A. Gasteiger, "Handbook of Fuel Cells Fundamentals, Technology and Applications", Volume 2, John Wiley & Sons Ltd., New York, 2005.
- [3] S.A. Grigoriev; V.N. Fateev J. Power Sources 245,112 (2008).
- [4] S. Martinez, M. Metikos-Hukovic, L. Valek., J. Mol. Catal. A: Chem 245,114 (2006).
- [5] L. Sanchez, S. Domingues, C. Marino, L. Mascaro., Electrochem. Comm. 6, 543 (2004).
- [6] I. A. Raj; K.I. Vasu J. Applied Electrochem. 20, 32 (1990).
- [7] L. Huang, F. Yang, S. Xu, S. Zhou., T. I. Met. Finish. 79, 136 (2001).
- [8] R. Schulz; J.Y. Hout; M.L. Trudeau; L. Dignard-Bailey; Z.H. Yan, J. Mater. Res. 9, 2998 (1994).
- [9] G. Martínez; G. Zavala; M. Videa J. Mex. Chem. Soc. 53, 7 (2008).
- [10] M. Obradovic; R. Stevanovic; A. Despic., J. Electroanal. Chem. 552, 185 (2003).
- [11] V.V. Kunznetov; N.V. Morozova; V. Kudryavtsev., Russ. J. Electrochem. 42, 665(2006).
- [12] J.G. Highfield, E. Claude, K. Oguro, Electrochim. Acta 44, 2805 (1999).
- [13] E. Chassaing, N. Portail, A. Levy, G. Wang., J. Appl. Electrochem. 34, 1085 (2004).
- [14] M.P. Zach and R.M. Penner, Adv. Mat., 12, 878 (2000).
- [15] M. Donten; H. Cesiulis ; Z. Stojek., Electrochimica Acta 50, 1405 (2005).
- [16] J. Crousier, M. Eyraud, J.-P. Crousier, J. Appl. Electrochem. 22, 749 (1992).